Experimental Eye Research 91 (2010) 369–377

Contents lists available at ScienceDirect

Experimental Eye Research

journal homepage: www.elsevier.com/locate/yexer

Evolution of damage in the lens after *in vivo* close to threshold exposure to UV-B radiation: Cytomorphological study of apoptosis

Konstantin Galichanin [a,b,*], Stefan Löfgren [a], Jan Bergmanson [c], Per Söderberg [b]

[a] St. Erik's Eye Hospital, Karolinska Institutet, Stockholm, Sweden
[b] Gullstrand Lab, Ophthalmology, Department of Neuroscience, Uppsala University Hospital, Uppsala, Sweden
[c] Texas Eye Research and Technology Center, University of Houston College of Optometry, Houston, Texas, USA

ARTICLE INFO

Article history:
Received 14 May 2010
Accepted in revised form 10 June 2010
Available online 17 June 2010

Keywords:
lens
ultraviolet radiation
cataract
apoptosis
repair
light scattering
microscopy

ABSTRACT

The purpose of the present study was to investigate cataractogenesis and recovery of lens damage after *in vivo* close to threshold ultraviolet (UV)-B radiation around 300 nm. Eighty six-week-old albino Sprague–Dawley rats were familiarized to a rat restrainer five days prior to exposure. Groups of non-anesthetized rats were exposed unilaterally to 8 kJ/m^2 UVR-300 nm. The animals were sacrificed at 1, 7, 48 and 336 h following exposure. The lenses were extracted for imaging of dark-field lens macro anatomy and measurement of intensity of forward lens light scattering to quantify lens opacities. Three exposed lenses and one non-exposed lens from each time interval were examined with light and transmission electron microscopy (TEM). Macro anatomy and lens light scattering revealed that all contralateral non-exposed lenses were clear. The degree of lens opacity (difference in lens light scattering between exposed and non-exposed lenses) increased during the 336 h, reaching a plateau towards the end of the observation period. Light microscopy and TEM demonstrated that apoptotic features appeared in the epithelium already 1 h after UVR exposure, and small vacuoles were seen in the outer cortex. Epithelial damage occurs during the first 48 h after exposure and is followed by regenerative repair at 336 h post-exposure. Apoptotic epithelial cells were phagocytized by adjacent epithelial cells. Cortical fiber cells exhibited increasing damage throughout the observation period without any clear repair after 336 h. In conclusion, acute UVR-induced cataract is partly a reversible. Lens epithelium is a primary target for UVR exposure. Damage to cortical fiber cells remained irreversible.

1. Introduction

Cataract is the number one cause of blindness in the world (Brian and Taylor, 2001; Evans et al., 2004; West, 2000). Phacoemulsification is the most prevalent cure of cataract in developed countries (Asbell et al., 2005). In spite of the progress made in cataract surgical techniques and materials during the last ten years, cataract continues to be a substantial public-health issue globally (Resnikoff et al., 2004). The Eye Disease Prevalence Research Group has projected that the number of US patients with cataract will increase by 50% by 2020 (Congdon et al., 2004). To join the efforts for blindness prevention the World Health Organization with other institutions has launched the Global Initiative for the Elimination of Avoidable Blindness "VISION 2020: the Right to Sight" (Thylefors, 1998). The magnitude of the cataract problem emphasizes the importance of development of cataract prevention and treatment strategies.

Solar radiation is the major source of UVR (Pitts, 1990). Exposure to sunlight has been correlated with the development of human senile cataract (Hiller et al., 1977; Italian–American Cataract Study, 1991; West and Valmadrid, 1995). Population-based studies in United States (Cruickshanks et al., 1992; Taylor et al., 1988), Australia (McCarty et al., 2000) and Japan (Sasaki et al., 2003) reported association between exposure to UVR-B and cortical cataract formation. Moreover, animal models have proven that exposure to UVR-B induces cataract (Jose and Pitts, 1985; Löfgren et al., 2003; Meyer et al., 2008; Michael et al., 1996; Pitts et al., 1977; Söderberg, 1988; Wegener, 1995).

The vertebrate ocular lens is a highly organized, compact and transparent structure that has evolved to refract light entering the eye. The lens comprises densely packed fibers and a single layer of epithelial cells on its anterior surface, enclosed by a thick elastic lens capsule. The entire homeostasis, in which the lens develops, differentiates and grows throughout life, is maintained by all the

* Address correspondence to: Konstantin Galichanin, Gullstrand Lab, Ophthalmology, Dept. of Neuroscience, Uppsala University Hospital, SE-751 85 Uppsala, Sweden. Tel.: +46 18 611 3716; fax: +46 18 50 48 57.
E-mail address: konstantin.galichanin@neuro.uu.se (K. Galichanin).

0014-4835/$ – see front matter © 2010 Elsevier Ltd. All rights reserved.
doi:10.1016/j.exer.2010.06.009

parts. (Kuszak and Costello, 2004) The essential structure-function regimen of the lens can be altered by environmental factors such as UVR radiation (Hightower, 1995; Zigman, 1985). UVR-B photons damage both the lens epithelium and the lens fiber cells by different mechanisms. In the lens epithelial cells, UVR-B irradiation leads to unscheduled DNA synthesis (Söderberg et al., 1986), formation of pyrimidine dimmers, DNA-DNA and DNA-protein cross linking, DNA single and double strand breaks (Kleiman et al., 1990), perturbation of calcium cell signaling and decline in reduced glutathione (Hightower et al., 1999), Na/K-ATPase inhibition (Hightower and McCready, 1992), increased membrane permeability (Hightower et al., 1994) and alterations in protein synthesis (Andley et al., 1990). In the lens fiber cells, UVR-B causes aggregation of lens crystallins (Zigman et al., 1973), photolysis of human lens α-crystallin and generation of reactive oxygen species (Andley and Clark, 1989), mitochondrial rounding and movement cessation (Bantseev and Youn, 2006).

Besides all the above-listed molecular processes, apoptosis plays a critical role in initiation of cataract in humans and animals (Li et al., 1995). The term apoptosis was first used by Kerr et al. in 1972 to describe the morphological alterations of certain forms of programmed or physiological cell death (Kerr et al., 1972). Transmission electron microscopy is the gold standard to confirm apoptosis and distinguish it from necrosis. Morphologically, apoptosis is characterised by a condensation of both nuclear chromatin (karyopyknosis) and cytoplasm, which is followed by fragmentation of the nucleus (karyorhexis) and formation of apoptotic bodies containing nuclear material and closely packed cell organelles. Formed apoptotic bodies can be phagocytosed by macrophages or by adjacent cells and subsequently shed from epithelial surfaces. There is no inflammatory reaction in apoptosis (Elmore, 2007).

Apoptosis is a morphologically and biochemically distinct mode of programmed cell death which is genetically regulated and energy dependent. The two best understood signaling apoptotic pathways in mammalian cells are the extrinsic or death receptor pathway and the intrinsic or mitochondrial pathway. Cells exposed to UVR undergo apoptosis through the intrinsic pathway, causing DNA fragmentation and condensation of nuclear chromatin (Elmore, 2007). Exposure to UVR causes apoptosis in the lens epithelial cells in vitro (Li and Spector, 1996; Long et al., 2004). In our research group, apoptosis has been investigated after in vivo UVR 300 nm exposure to the lens (Michael et al., 1998) and was found to be mediated by increased expression of p53 (Ayala et al., 2007).

Previously Söderberg revealed the sequence of microscopical events underlying cataractogenesis after high dose exposure to UVR 300 nm (Söderberg, 1988). Those events could be due to apoptosis. The threshold dose for UVR cataract was later found to be ten-fold lower than the dose used in the 1988 investigation (Söderberg et al., 2002). It is consequently important to investigate whether the morphology of cataract after close to threshold UVR is similar to that at ten times threshold, and to demonstrate chronology of apoptotic features in the lens.

2. Materials and methods

Non-anesthetized animals were exposed unilaterally in vivo to UVR-B. The intensity of forward lens light scattering was measured in vitro at incrementing post exposure intervals. The lens morphology was studied by light and transmission electron microscopy.

2.1. Animals

Eighty six-week-old albino Sprague–Dawley (SD) female rats (Scanbur BK AB, Sollentuna, Sweden) were treated in accordance to the ARVO Statement for the Use of Animals in Ophthalmic and Visual Research. Ethical approval was obtained from the Northern Stockholm Animal Experiments Ethics Committee, protocol number N184/04.

2.2. Exposure to ultraviolet radiation

2.2.1. UVR source

UVR-B in the 300 nm wavelength region was generated with a high-pressure mercury lamp (model 6828; Oriel, Stratford CT). The emerging radiation was collimated, passed through a water filter and focused into a double monochromator, set to deliver a spectrum centered at 300 nm with dual peaks at 207.5 nm and 302.6 nm (due to strong mercury lines near 300 nm) and 10.2 nm full width at half maximum (Galichanin et al., 2010).

2.2.2. UVR exposure

Five days prior to exposure all rats were conditioned and fixed to a newly developed rat restrainer (Galichanin et al., 2010). Each non-anesthetized animal was exposed unilaterally to double threshold dose 8 kJ/m^2 UVR-300 nm for 15 min (Söderberg et al., 2002), while the contralateral eye was shielded during exposure and used as internal control.

After a pre-determined post-exposure period, the rat was sacrificed by carbon dioxide asphyxiation, followed by cervical dislocation. The eyes were enucleated and the lenses were extracted. Remnants of the ciliary body were removed from the lens equator under a microscope, keeping the lens in balanced salt solution (BSS; Alcon, USA).

2.3. Quantification of lens opacification

The degree of lens opacification was quantified in vitro by measurement of intensity of forward lens light scattering with a light dissemination meter (Söderberg et al., 1990).

2.4. Macroscopic imaging

Thereafter, the macroscopic appearance of the lens was documented with digital photography in incident illumination against a grid and in dark field illumination.

2.5. Light and transmission electron microscopy

After macro photography samples of 4 lenses from each post-exposure time interval were fixed in a 0.08 M cacodylate-buffered solution of 1.25% glutaraldehyde and 1% paraformaldehyde (pH 7.3) for at least 7 days at 4 °C. After that, the lenses were dissected into equatorial rim, anterior and posterior surfaces, and furthermore divided into 2 similar halfs (6 specimens per lens). Each piece of the lens was post-fixed in a 0.1 M cacodylate buffered solution of 1% osmium tetroxide supplemented with 1.5% potassium ferricyanide for 1 h at 4 °C and thereafter dehydrated in a graded series of ethanol up to 100%, and embedded in epoxy resin.

Semithin sections of the embedded lens tissue were stained with 1 % toluidine blue for light microscopy. Ultrathin sections were obtained and mounted on parallel bar copper grids. The sections were then double stained in 3.5 % uranyl acetate for 20 min at room temperature, followed by Reynold's lead citrate for 10 min at room temperature. The grids with sections were examined in a Tecnai G2 Bio Twin Spirit (FEI Company, USA) transmission electron microscope.

2.6. Experimental design

Altogether, 80 SD rats were randomly distributed in four latency groups of 20 animals each: 1, 7, 48 and 336 h. These time intervals were selected in a geometric scale because development of lens light scattering has an exponential regression trend (Söderberg, 1990). One eye in each animal was exposed to UVR-300 nm and the intensity of light scattering was measured 3 times for each lens after the post-exposure interval indicated by the group assignment.

2.7. Statistics

The significance level and the confidence coefficients were, considering the sample size and the expected contrasts, set to 0.05 and 0.95, respectively. The paired difference in light scattering between exposed and contralateral lens was used as primary data in the analyses. It was a priori decided to analyze contrast between post-exposure intervals with orthogonal comparisons according to the scheme: 336 h versus 48 h, 336 h and 48 h versus 7 h, and 336 h, 48 h and 7 h versus 1 h.

3. Results

3.1. Evolution of intensity of forward light scattering

The difference of light scattering increased exponentially declining with increasing post-exposure time (Fig. 1).

The variances for the various post-exposure intervals were compared with Bartlett's test and found to vary (test statistic = 114.8, $\chi^2_{3;0.05} = 7.81$). For this reason, orthogonal t-tests were used for the orthogonal testing of contrasts among post-exposure intervals. Orthogonal comparison between the different post-exposure intervals revealed that there is no difference of light scattering induced between 336 and 48 h (test statistic = 0.92, $t_{0.95;38} = 2.02$), there is a difference of light scattering induced between 336 h and 48 h versus 7 h (test statistic = 3.43, $t_{0.95;58} = 2.00$), and there is a difference of light scattering between 336 h, 48 h and 7 h versus 1 h (test statistic = 2.75, $t_{0.95;78} = 1.99$).

Considering the outcome of the orthogonal *t*-tests, the differences of intensity of light scattering, I_d, as a function of post-exposure interval, t, were fitted to a first order exponential regression model, assuming an increase of light scattering towards an asymptote, I_i, and an increase rate, k (Equation (1)).

$$I_d = I_i\left(1 - e^{-kt}\right) \quad (1)$$

The lens light scattering increased, with an exponential decline, with an increase rate of 0.02 h^{-1} corresponding to a time constant ($1/k$) of 47 h and asymptote maximum light scattering of 0.16 tEDC (Fig. 1). The squared regression coefficient was 0.91.

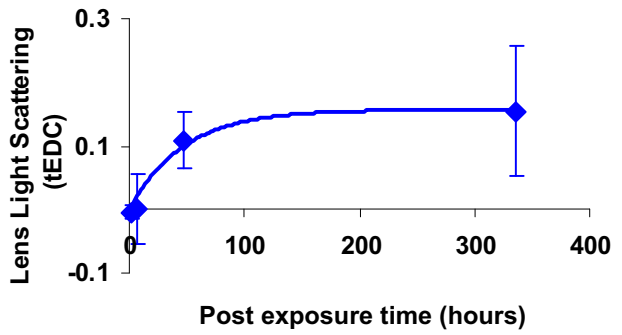

Fig. 1. Evolution of difference of forward lens light scattering after in vivo exposure to 8 kJ/m^2 UVR at 300 nm. Error bars are 95% confidence intervals for the mean. The line shows best fit to an exponential regression model.

3.2. Macroscopic appearance

Non-exposed lenses from all groups were clear and transparent with smooth surface (Fig. 2).

The first macroscopic changes in the UVR-exposed lenses appeared at 7 h, as a slight haze in the epithelium with accentuation of the sutures (Fig. 3).

After 48 h prominent dot-like opacities were seen in the epithelium with a concentric demarcation line near the equator. At 336 h the lens was again clear with the exception of small vacuoles (50–100 μm) in the equatorial cortex.

Three exposed lenses in the 336 h group developed severe cataract, two of them with cortical cataract and one with both cortical and nuclear cataract (Fig. 4).

3.3. Light and transmission electron microscopy

Sections of control lenses demonstrated a normal single layer of epithelial cells, regular architecture of the nuclear bow, and the lens fibers were packed and oriented in order (Figs. 5 and 6).

One hour after UVR exposure, irregular epithelial cells occasionally appeared in the central zone (Fig. 3, 1 h: LM-A), but no disturbances were found in other areas of the epithelium. In ultrastructure, irregular epithelial cells in the central zone showed apoptotic features (Fig. 3, 1 h: TEM-A). The nuclear bow (Fig. 3, 1 h: LM-B) and equatorial epithelial cells (Fig. 3, 1 h: TEM-B) appeared normal. The outer posterior cortex showed small vacuoles (Fig. 3, 1 h: LM-C). Ultrastructurally, superficial lens fiber cells in the anterior, equatorial and posterior cortex had regular structure but there were extracellular vacuoles anteriorly (Fig. 3, 1 h: TEM-A) and posteriorly. Deeper fiber cells had normal morphology throughout the whole cell length.

At 7 h post-exposure, irregularly shaped epithelial cells occurred all over the central epithelial zone (Fig. 3, 7 h: LM-A). The nuclear bow and the posterior region of the lens appeared normal (Fig. 3, 7 h: LM-B and C). Transmission electron microscopy revealed that apoptotic cells exhibited chromatin condensation, intact cell membrane and cell convolution (Fig. 3, 7 h: TEM-A). Towards the equator, the epithelium became normal in appearance (Fig. 3, 7 h: TEM-B). The fiber order was disturbed in the outer anterior cortex while equatorial fibers appeared normal (Fig. 3, 7 h: LM-B) but there were abundant vacuoles in the superficial posterior cortex (Fig. 3, 7 h: LM-C). Deeper fiber cells were hexagonal in transverse section and arranged in typical order.

At 48 h after exposure, there were areas missing epithelial cells and remaining epithelial cells contained nuclear and cytoplasmic condensations, exhibiting apoptotic appearance, and were aggregated in multiple layers (Fig. 3, 48 h: LM-A). TEM verified that the epithelium was full of cells with apoptotic bodies, debris and extracellular spaces (Fig. 3, 48 h: TEM-A). The nuclei of these cells were fragmented and with dense chromatin. The membranes of the epithelial cells were intact. Closer to the nuclear bow region, epithelial cells aggregated in multiple layers (Fig. 3, 48 h: TEM-B). Epithelial cells surrounding a target cell through the extensions of pseudopodia and fusing its pseudopodia to engulf apoptotic bodies, resulting in formation of a phagosome or phago-lysosome, phagocytosis, was observed (Fig. 7).

The nuclear bow was deteriorated and cortical fiber cells appeared swollen, partly fused and contained vacuoles (Fig. 3, 48 h: LM-B). In the posterior subcapsular area vacuoles were abundant (Fig. 3, 48 h: LM-C). Looking at TEM, superficial fiber cells were heavily swollen and fused with disturbed orientation and numerous vacuoles, while deeper fiber cells remained accurately organized.

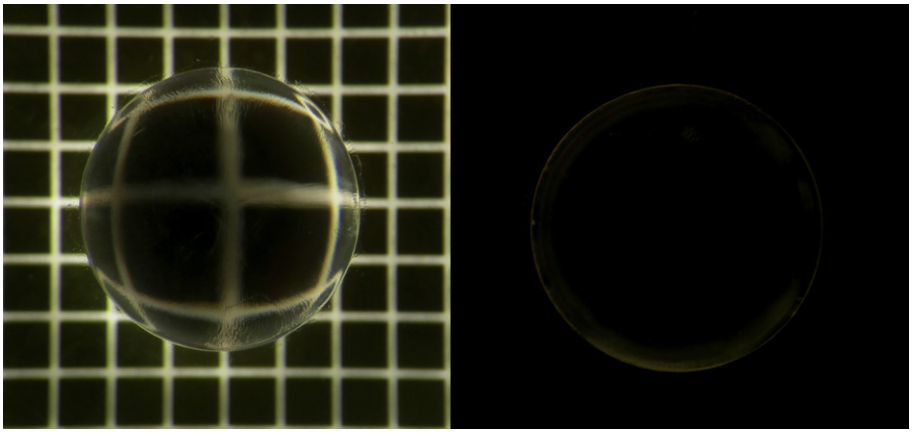

Fig. 2. Contralateral non-exposed lenses in bright-field (left) and dark-field (right) illumination. Grid square diameter is 0.79 mm.

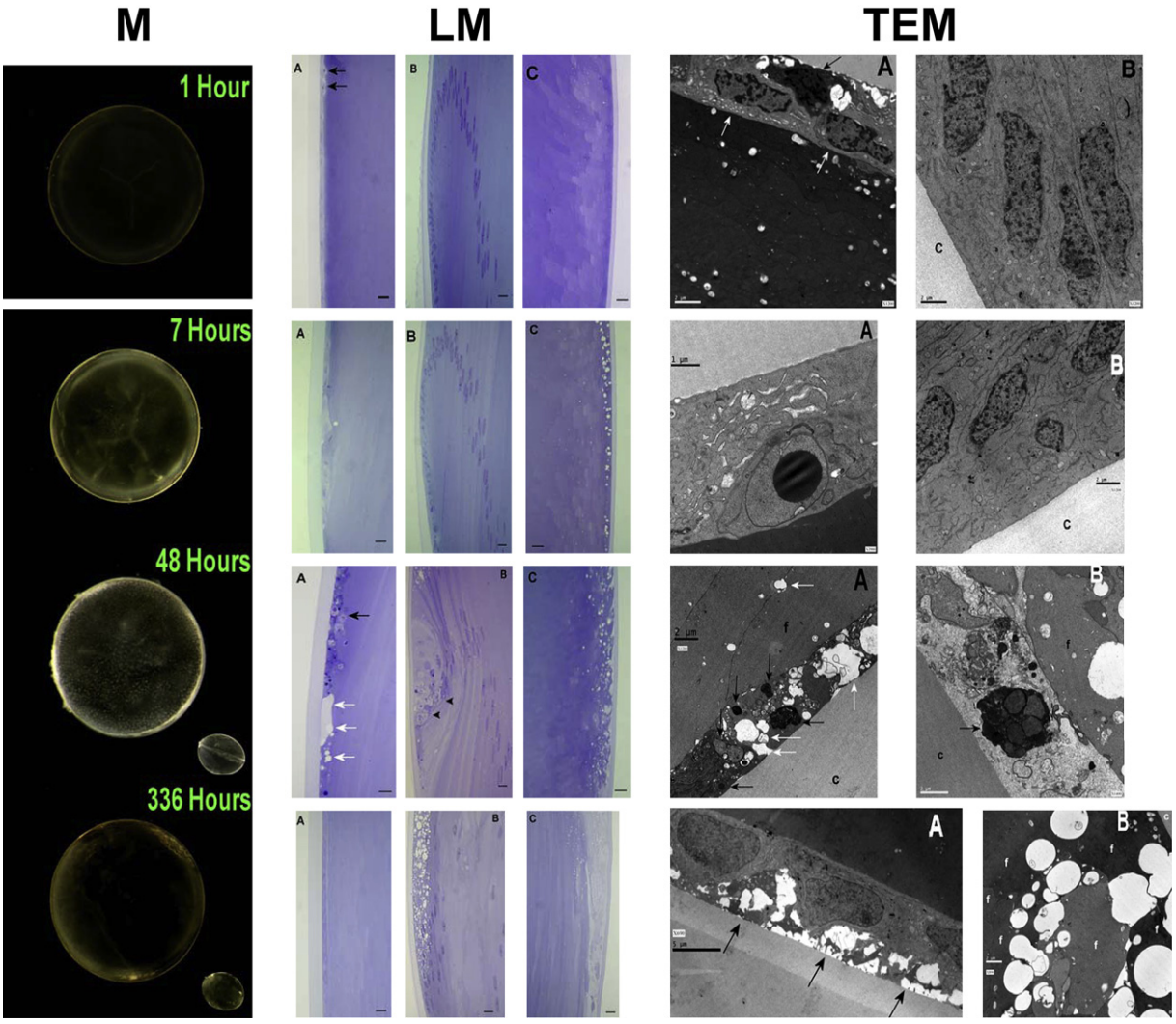

Fig. 3. Macrographs (M) of lenses in dark-field illumination (column 1); light micrographs (LM) of central epithelial zone (column 2), nuclear bow region (column 3) and posterior region (column 4). Scale bar is 10 μm. Transmission electron micrographs (TEM) of lens epithelium (column 5) and nuclear bow region (column 6) after in vivo exposure to UVR. At 1 h after exposure to UVR: LM-A, arrowheads indicate apoptotic epithelial cells with karyopyknosis, TEM-A, one apoptotic cell with condensed cytoplasm (black arrow) among two normal epithelial cells (white arrow). TEM-B, elongating normal epithelial cells at transitional zone. At 7 h after exposure to UVR: TEM-A, rounding apoptotic cell with karyopyknosis and intact cell membrane. TEM-B, normal epithelial cells at transitional zone. At 48 h after exposure to UVR: LM-A, multilayering of the central epithelium and apoptotic cells detached from capsule (black arrowhead), loss of the epithelial cells (white arrowheads). LM-B, apoptotic bodies and debris disintegrating nuclear bow (black arrows). TEM-A, apoptotic bodies (black arrowheads), vacuoles (white arrows); c – capsule, f – fiber cells. TEM-B, debris of several apoptotic bodies (arrow). At 336 h after exposure to UVR: TEM-A, normal epithelial cells with subcapsular vacuoles (black arrows). TEM-B, swollen fiber cells with large extracellular granules; c – capsule, f – fiber cells.

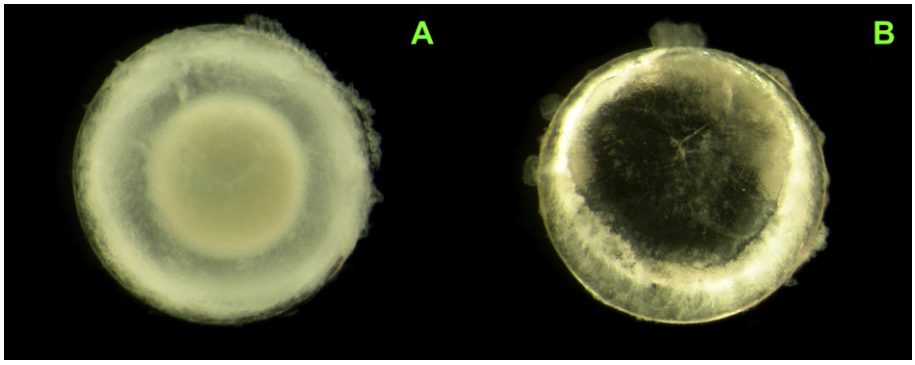

Fig. 4. UVR-exposed lens with nuclear and cortical cataract (A) and cortical cataract (B). Dark-field illumination photography.

At 336 h after UVR exposure, the epithelium returned to a monolayer of cells (Fig. 3, 336 h: LM-A) but there was frequently accumulations of vacuoles between the epithelial cells and the capsule (Fig. 3, 336 h: TEM-A). The cortical fiber cells were still damaged, without any clear sign of repair (Fig. 3, 336 h: LM-B, TEM-B). The superficial anterior cortex had swollen and heavily fused fiber cells. The superficial equatorial cortex was composed of disoriented, heavily swollen fiber cells with large intercellular vacuoles. The posterior outer cortex exhibited swollen and disorganized fiber cells (Fig. 8).

No alterations of the lens capsule were detected after the exposure to UVR. The lens nucleus could not be evaluated because it became opaque after fixation and crumbled during sectioning.

4. Discussion

This study investigated the evolution of cataract and chronology of apoptotic events in the lens after in vivo exposure to close to threshold dose of UVR.

4.1. Lens opacification

Light scattering increases exponentially after exposure to 8 kJ/m^2 (Fig. 1), similar to the response to 30 kJ/m^2 (Fig. 9) (Söderberg, 1990).

However, at the lower dose the onset was slower and the level of light scattering was lower. In other words, lens light scattering evolves quicker with higher UVR dose and reaches a higher level. Moreover, the method of animal immobilisation, either restraining as in the current experiment or anesthesia as in the foregoing study (Söderberg, 1990) does not alter the exponential trend of lens forward light scattering (Fig. 9). The higher level of long term light scattering induced with a higher dose is consistent with previous findings demonstrating a continuous dose response relationship between dose of UVR and induced long term light scattering (Söderberg et al., 2003).

An analysis of the high variability of light scattering difference for the 336 h post exposure interval (Fig. 1) demonstrated that three animals expressed a large difference of light scattering, 0.6–0.7 tEDC, between exposed and contralateral not exposed lens, while the other animals expressed a lower difference (Fig. 10).

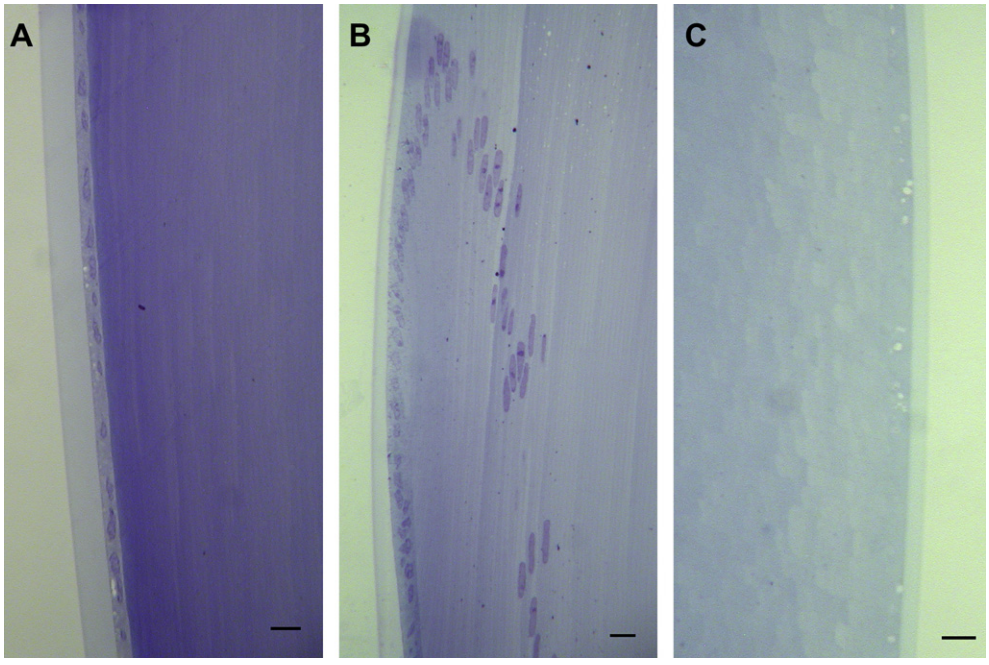

Fig. 5. Sagittal sections of non-exposed rat lens. Central epithelial zone (A), nuclear bow region (B) and posterior region (C). Scale bar is 10 μm.

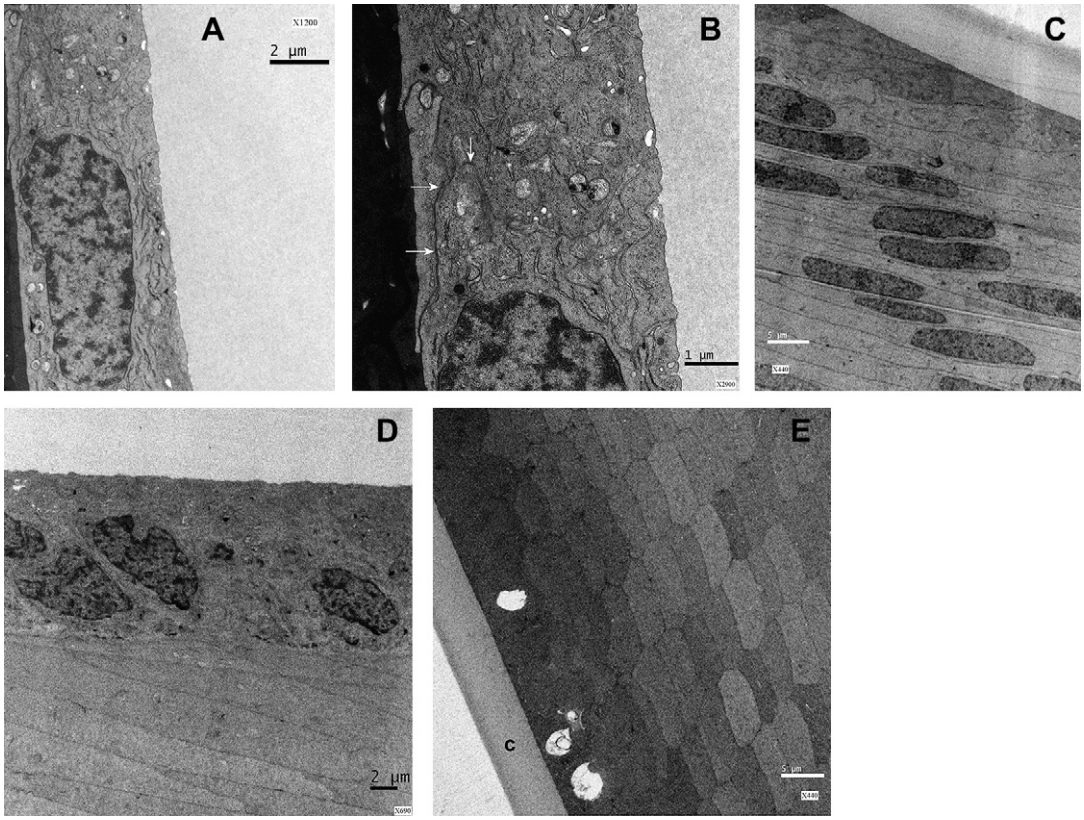

Fig. 6. Transmission electron micrographs of non-exposed lens epithelium (A,B), nuclear bow region (C,D) and posterior region (E). Intact epithelial cell membrane is indicated with white arrows (B). Normal order of lens fiber cells (C). Epithelial cells at germinative zone (D). Normal lens fiber cells showing hexagonal shapes in normal order, c – capsule (E).

Two of the lenses in the 336 h group, expressed severe cortical cataract and one lens expressed both nuclear and cortical cataract, in addition to anterior subcapsular cataract (Fig. 4). Our research group has repeatedly reported this variable expression of cataract (Dong et al., 2003; Löfgren et al., 2003; Meyer et al., 2008, 2005). The variable expression of cataract could be due to varying repair capacity (Meyer et al., 2005). We hypothesize that the repair system of the lens is overloaded in more sensitive animals, leading to

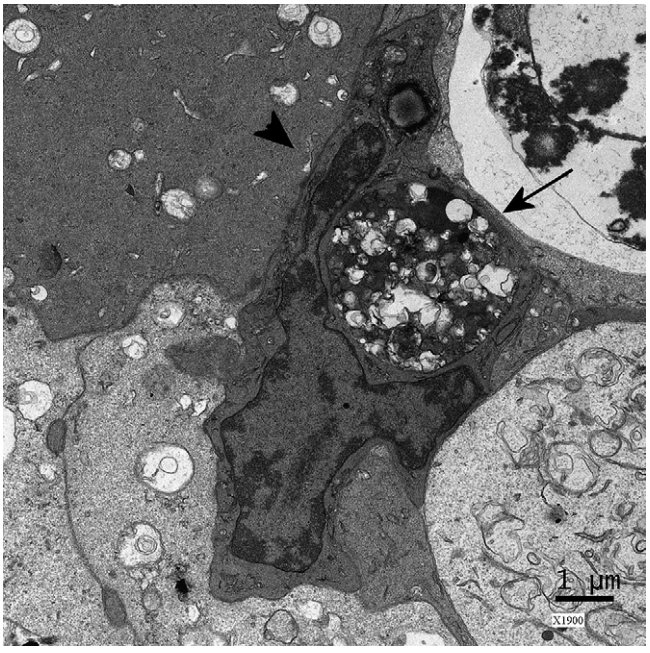

Fig. 7. Transmission electron micrograph of epithelial cell (arrowhead) 48 h post-exposure with engulfed debris of apoptotic bodies in a phagosome (arrowhead).

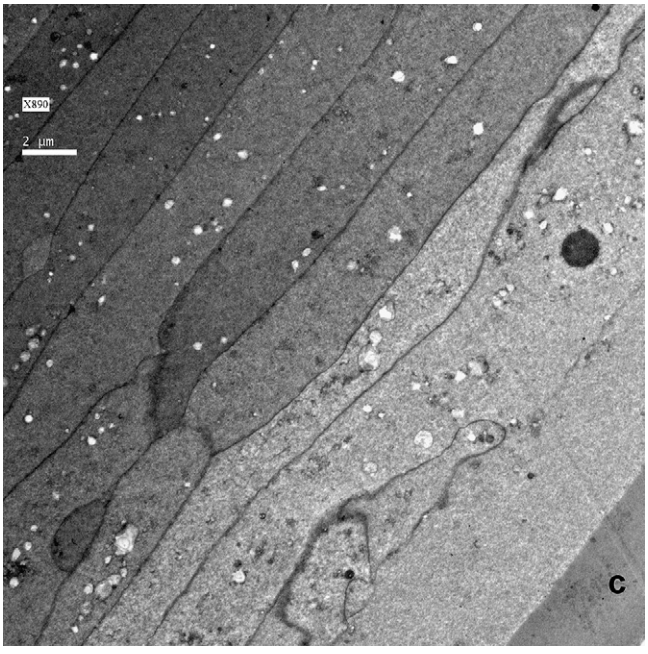

Fig. 8. Longitudinal ultrathin section of posterior lens fiber cells 336 h post-exposure, showing swollen appearance. c – capsule.

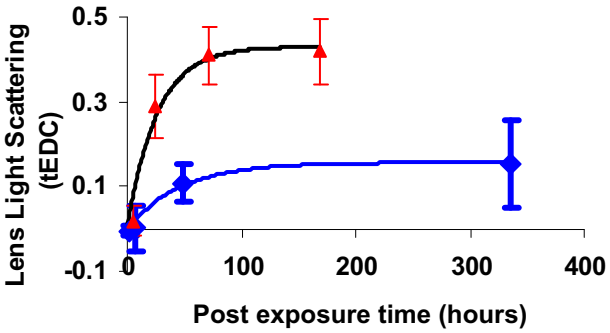

Fig. 9. Mean paired lens light scattering after in vivo exposure to 8 kJ/m^2 ◆ and to 30 kJ/m^2 ▲ UVR-300 nm. Error bars are 95% confidence intervals. The lines show best fit to exponential regression model.

manifest severe cataract, while in other animals the repair system reduces the cataract expressed. The fact that severe cortical (in 2 out of 20 lenses) and both cortical and nuclear (in 1 out of 20 lenses) cataract was seen in exposed lenses only in the 336 h group indicates that there may be a critical time point between 48 h and 336 h at which it is determined whether the repair system has been overloaded or will reduce the damage expressed.

An alternative explanation to the large variability in sensitivity observed at 336 h is that the actual dose of UVR received was higher in some animals. This seems highly unlikely since the irradiance of the source was verified before and after exposure, the radiometer used is highly stable over extended periods of time and regularly calibrated.

Administration of ketamine-xylazine anesthesia can induce acute transient lens opacities in rats and mice (Calderone et al., 1986) (Zhang et al., 2007). The acute transient lens opacity due to ketmaine-xylazine anesthesia usually starts within 1 h after induction and clears within a few hours after induction, regardless of whether the stimulus is continued (Fraunfelder and Burns, 1966, 1970). In the present study, we used a rat restrainer (Galichanin et al., 2010) to avoid any transient opacities caused by anesthesia.

4.2. Macroscopic appearance

In similarity with other animal studies on UVR-induced cataract (Löfgren et al., 2003; Meyer et al., 2008; Michael et al., 2000; Söderberg, 1988; Wegener, 1994; Wu et al., 1997) we observed anterior subcapsular cataract in most of the lenses exposed to UVR. This is consistent with the fact that UV-B photons are attenuated superficially in the lens (Dillon, 1991; Dillon et al., 1999; Löfgren and Söderberg, 2001) and therefore primarily damage anterior lens parts (Hightower et al., 1994).

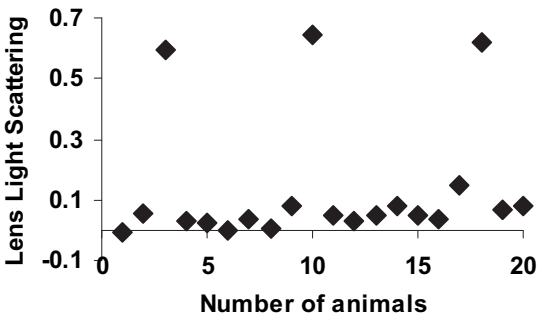

Fig. 10. Difference of light scattering between lens in vivo exposed to 8 kJ/m^2 UVR-300 nm and it's contralateral not exposed lens at 336 h after exposure.

4.3. Light and transmission electron microscopy

Macroscopically seen flake like opacities on the anterior surface of the lens are considered to be related to apoptotic changes in the lens epithelium (Michael et al., 2000). In this study we observed apoptosis already 1 h after in vivo exposure to UVR 300 nm (Fig. 3, 1 h: LM-A, TEM-A). However the exposed lens was macroscopically almost as transparent as a not exposed control lens up to 7 h after exposure (Figs. 2 and 3, 1 h and 7 h: M). Söderberg et al. (Söderberg, 1988) observed apoptotic-like changes in the epithelium at 1 h after in vivo exposure to approximately 10 times threshold dose (Söderberg et al., 2002), whereas no macroscopic changes could be detected. At 6 h post-exposure they found anterior flake like opacities (Söderberg, 1988). These in vivo findings corroborate observations of in vitro cultured lenses that were exposed to broadband UVR (Li and Spector, 1996). That study indicated that apoptosis, assayed by TUNEL labelling, precedes macroscopic appearance of anterior lenticular opacities and increases up to 24 h after exposure. Michael et al. (1998) were only able to detect TUNEL labelling at 24 h after in vivo exposure to 5 kJ/m^2. The lack of TUNEL labelling at shorter post-exposure intervals may have been due to low sensitivity. Ayala et al. (Ayala et al., 2007) observed an increase of p53 and caspase 3 expression on mRNA and protein levels at 1 week after in vivo exposure to 8 kJ/m^2 of UVR-B. The latter finding suggests that the apoptotic mechanism acts up to at least 1 week after exposure.

Li and Spector (Li and Spector, 1996), using 9 kJ/m^2 and 28.8 kJ/m^2 exposure of in vitro cultured lenses further observed that appearance of apoptosis in lens epithelial cells is earlier the higher the UVR dose. We currently observed that the onset of light scattering is quicker, the higher the exposure dose (Fig. 9). Thus, apoptosis precedes expression of light scattering and with the higher the exposure dose, the earlier the appearance of apoptosis and the higher the increase rate of light scattering.

Our observation of phagocytosis at 48 h after exposure (Fig. 7) is consistent with previous findings in in vivo UVR exposed lenses (Michael et al., 1998). Our observation of phagocytosis also fits with results showing that phagocytosis plays a prominent role in elimination of degraded products in the last stage of apoptosis (Arends and Wyllie, 1991; Kerr et al., 1972). The time from initiation of apoptosis to completion with phagocytosis can vary significantly (Arends and Wyllie, 1991). Not all stages of phagocytosis such as chemotaxis can be visualized by TEM and further investigations are required to determine the time course of phagocytosis from early to later stages after UVR-B exposure.

The finding of small extracellular vacuoles between epithelial cells at 1 h after in vivo exposure to UVR (Fig. 3, 1 h: TEM-A) and large extracellular equatorial spaces at 336 h post-exposure (Fig. 3, 336 h: LM-B, TEM-B) indicates that the exposure to UVR induced an osmotic disturbance in the lens. This is consistent with previous findings (Söderberg, 1991). Those large vacuoles may be related to extracellular accumulation of calcium, a major source of light scatter (Vrensen et al., 1995). Extracellular vacuoles and deteriorated fiber cells are likely to give increase in lens light scattering after 336 h post-exposure (Fig. 9).

We hypothesize that apoptotic loss of epithelial cells as a consequence of the UVR-exposure causes osmodisregulation that impairs the metabolic activity of the outer lens fiber cells. This imbalance propagates through ion (Duncan, 1969) and macromolecular pathways (Shestopalov and Bassnett, 2000) into the deeper cortex. If outer lens fiber cells are disturbed by frontal exposure to UVR, it will result in metabolic disorders in deeper fiber cells through fiber cell membrane fusions (Duncan, 1969; Shestopalov and Bassnett, 2000). These cell–cell communications explain why the first swollen fiber cells were found in the anterior outer cortex at 7 h post-exposure (Fig. 3, 7 h: LM-A), subsequently followed by

disintegration of fiber cells all over the outer cortex at 48 h post-exposure (Fig. 3, 48 h: LM) and continued damage into the deeper cortex at 336 h post-exposure (Fig. 3, 336 h: LM).

During normal lens growth, epithelial cells in the germinative zone proliferate and differentiate into fiber cells, while daughter cells migrate and contribute to the epithelial monolayer (Rafferty and Rafferty, 1981). The return of the epithelium to a monolayer of cells 336 h following UVR exposure (Fig. 3, 336 h: LM-A) may be due to UVR triggered mitotic activity of stem cells within the germinative zone. Such daughter cells may have repopulated central zone area where epithelial cells were lost, thus recovering lens capsule left naked or with remnants of cells that had undergone apoptosis (Fig. 3, 336 h: TEM-A).

5. Conclusion

The higher the in vivo UVR dose, the faster the development of lens opacification and the higher the end level of lens opacification. Lens epithelial cells appear to be the primary target for UVR exposure. Apoptotic events in the epithelium precede, both temporally and spatially, macroscopic cataractogenesis. Epithelial damage occurs during the first 48 h after exposure and is followed by regenerative repair at 336 h post-exposure. Damage to cortical fiber cells remained irreversible.

Acknowledgements

The authors thank Monica Aronsson for professional animal care, Dr. Linda Meyer for helpful discussions, Berit Spångberg for technical assistance with light microscopy and Margaret Gondo for help with electron microsopy imaging. The paper was presented in part as an abstract at the Association for Research in Vision and Ophthalmology Congress 2008. This work was supported by the Karolinska Institutet KID-funding, Swedish Radiation Protection Authority, Karolinska Institutet Eye Research Foundation, Karolinska Institutet Research Foundation, Gun och Bertil Stohnes Stiftelse, Swedish Research Council; project K2006-74X-15035-03-2, K2008-63X-15035-05-2, Konung Gustav V:s och Drottning Victorias Frimurarstiftelse.

References

Andley, U.P., Clark, B.A., 1989. Generation of oxidants in the near-UV photooxidation of human lens a-crystallin. Investigative Ophthalmology and Visual Science 30, 706–713.
Andley, U.P., Walsh, A., Kochevar, I.E., Reddan, J.R., 1990. Effect of ultraviolet-B radiation on protein synthesis in cultured lens epithelial cells. Current Eye Research 9, 1099–1106.
Arends, M.J., Wyllie, A.H., 1991. Apoptosis: mechanisms and roles in pathology. International Review of Experimental Pathology 32, 223–254.
Asbell, P.A., Dualan, I., Mindel, J., Brocks, S., Ahmad, M., Epstein, S., 2005. Age related cataract. Lancet 365, 599–609.
Ayala, M.N., Strid, H., Jacobsson, U., Söderberg, P.G., 2007. p53 expression and apoptosis in the lens after ultraviolet radiation exposure. Investigative Ophthalmology of Visual Science 48, 4187–4191.
Bantseev, V., Youn, H.Y., 2006. Mitochondrial “movement” and lens optics following oxidative stress from. Annals of the New York Academy of Sciences 1091, 17–33.
Brian, G., Taylor, H.R., 2001. Cataract blindness: challenge for the 21 st century. Bulletin of the World Health Organization 79, 249–256.
Calderone, L., Grimes, P., Shalev, M., 1986. Acute reversible cataract induced by xylazine and by ketamine-xylazine anesthesia in rats and mice. Experimental Eye Research 42, 331–337.
Cruickshanks, K.J., Klein, B.E., Klein, R., 1992. Ultraviolet light exposure and lens opacities: the Beaver Dam Eye Study. American Journal of Public Health 82, 1658–1662.
Dillon, J., 1991. The photophysics and photobiology of the eye. Journal of Photochemistry and Photobiology B 10, 23–40.
Dillon, J., Zheng, L., Merriam, J.C., Gaillard, E.R., 1999. The optical properties of the anterior segment of the eye: implications for cortical cataract. Experimental Eye Research 68, 785–795.
Dong, X., Ayala, M., Löfgren, S., Söderberg, P.G., 2003. Ultraviolet radiation-induced cataract: age and maximum acceptable dose. Investigative Ophthalmology and Visual Science 44, 1150–1154.
Duncan, G., 1969. The site of the ion restricting membranes in the toad lens. Experimental Eye Research 8, 406–412.
Elmore, S., 2007. Apoptosis: a review of programmed cell death. Toxicologic Pathology 35.
Evans, J.R., Fletcher, A.E., Wormand, R.P., 2004. Causes of visual impairment in people aged 75 years and older in Britain: an add-on study to the MRC Trial of Assessment and Management of Older People in the Community. British Journal of Ophthalmology 88, 365–370.
Fraunfelder, F.T., Burns, R.P., 1966. Effect of lid-closure in drug-induced experimental cataracts. Archives of Ophthalmology 76, 599–601.
Fraunfelder, F.T., Burns, R.P., 1970. Acute reversible lens opacity: caused by drugs, cold, anoxia, asphyxia, stress, death and dehydration. Experimental Eye Research 10, 19–30.
Galichanin, K., Wang, J., Lofgren, S., Soderberg, P., 2010. A new universal rat restrainer for ophthalmic research. Acta Ophthalmologica.
Hightower, K., Duncan, G., Dawson, A., Wormstone, I., Reddan, J., Dziedzic, D., 1999. Ultraviolet irradiation (UVB) interrupts calcium cell signaling in lens epithelial cells. Photochemistry and Photobiology 69, 595–598.
Hightower, K., McCready, J., 1992. Mechanisms involved in cataract development following near-ultraviolet radiation of cultured lenses. Current Eye Research 11, 679–689.
Hightower, K.R., 1995. The role of the lens epithelium in development of UV cataract (Review). Current Eye Research 14, 71–78.
Hightower, K.R., Reddan, J.R., McCready, J.P., Dziedzic, D.C., 1994. Lens epithelium: a primary target of UVB irradiation. Experimental Eye Research 59, 557–564.
Hiller, R., Giacometti, L., Yuen, K., 1977. Sunlight and cataract: an epidemiologic investigation. American Journal of Epidemiology 105, 450–459.
Italian–American Cataract Study, G, 1991. Risk factors for age-related cortical, nuclear, and posterior subcapsular cataracts. American Journal of Epidemiology 133, 541–553.
Jose, J.G., Pitts, D.G., 1985. Wavelength dependency of cataracts in albino mice following chronic exposure. Experimental Eye Research 41, 545–563.
Kerr, J.F., Wyllie, A.H., Currie, A.R., 1972. Apoptosis: a basic biological phenomenon with wide-ranging implications in tissue kinetics. British Journal of Cancer 26, 239–257.
Kleiman, N.J., Wang, R., Spector, A., 1990. Ultraviolet light induced DNA damage and repair in bovine lens epithelial cells. Current Eye Research 9, 1185–1193.
Kuszak, J., Costello, M., 2004. The structure of the vertebrate lens. In: Lovicu, F., Robinson, M. (Eds.), Development of the Ocular Lens. Cambridge University Press, Cambridge, pp. 71–118.
Li, W.C., Kuszak, J.R., Dunn, K., Wang, R.R., Ma, W., Wang, G.M., Spector, A., Leib, M., Cotiar, A.M., 1995. Lens epithelial cell apoptosis appears to be a common cellular basis for non-congenital cataract development in humans and animals. Journal of Cell Biology 130, 169–181.
Li, W.C., Spector, A., 1996. Lens epithelial cell apoptosis is an early event in the development of UVB-induced cataract. Free Radical Biology and Medicine 20, 301–311.
Long, A.C., Colitz, C.M., Bomser, J.A., 2004. Apoptotic and necrotic mechanisms of stress-induced human lens epithelial cell death. Experimental Biology and Medicine (Maywood) 229, 1072–1080.
Löfgren, S., Michael, R., Soderberg, P.G., 2003. Impact of age and sex in ultraviolet radiation cataract in the rat. Investigative Ophthalmology and Visual Science 44, 1629–1633.
Löfgren, S., Söderberg, P.G., 2001. Lens lactate dehydrogenase inactivation after UV-B irradiation: an in vivo measure of UVR-B penetration. Investigative Ophthalmology and Visual Science 42, 1833–1836.
McCarty, C.A., Nanjan, M.B., Taylor, H.R., 2000. Attributable risk estimates for cataract to prioritize medical and public health action. Investigative Ophthalmology of Visual Science 41, 3720–3725.
Meyer, L., Dong, X., Wegener, A., Söderberg, P.G., 2008. Dose dependent cataractogenesis and Maximum Tolerable Dose (MTD 2.3:16) for UVR - B induced cataract in C57BL/6J mice. Experimental Eye Research 86, 282–289.
Meyer, L.M., Soderberg, P., Dong, X., Wegener, A., 2005. UVR-B induced cataract development in C57 mice. Experimental Eye Research 81, 389–394.
Michael, R., Söderberg, P.G., Chen, E., 1996. Long-term development of lens opacities after exposure to ultraviolet radiation at 300 nm. Ophthalmic Research 28, 209–218.
Michael, R., Vrensen, G., van Marle, J., Gan, L., Söderberg, P.G., 1998. Apoptosis in the rat lens after in vivo threshold dose ultraviolet irradiation. Investigative Ophthalmology and Visual Science 13, 2681–2687.
Michael, R., Vrensen, G.F.J.M., Marle, J.V., Löfgren, S., Söderberg, P.G., 2000. Repair in the rat lens after threshold ultraviolet radiation injury. Investigative Ophthalmology and Visual Science 41, 204–212.
Pitts, D.G., 1990. Sunlight as an ultraviolet source. Optometry and Vision Science 67, 401–406.
Pitts, D.G., Cullen, A.P., Hacker, P.D., 1977. Ocular effects of ultraviolet radiation from 295 to 365 nm. Investigative Ophthalmology and Visual Science 16, 932–939.
Rafferty, N.S., Rafferty Jr., K.I., 1981. Cell population kinetics of the mouse lens epithelium. Journal of Cellular Physiology 107, 309–315.
Resnikoff, S., Pascolini, D., Etya'ale, D., Kocur, I., Pararajasegaram, R., Pokharel, G.P., Mariotti, S.P., 2004. Global data on visual impairment in the year 2002. Bulletin of the World Health Organization 82, 844–851.
Sasaki, H., Kawakami, Y., Ono, M., Jonasson, F., Shui, Y.B., Cheng, H.M., Robman, L., McCarty, C., Chew, S.J., Sasaki, K., 2003. Localization of cortical cataract in subjects of diverse races and latitude. Investigative Ophthalmology and Visual Science 44, 4210–4214.

Shestopalov, V.I., Bassnett, S., 2000. Expression of autofluorescent proteins reveals a novel protein permeable pathway between cells in the lens core. Journal of Cell Science 113, 1913–1921.
Söderberg, P.G., 1988. Acute cataract in the rat after exposure to radiation in the 300 nm wavelength region. A study of the macro-, micro- and ultrastructure. Acta Ophthalmologica (Copenh) 66, 141–152.
Söderberg, P.G., 1990. Development of light dissemination in the rat lens after exposure to radiation in the 300 nm wavelength region. Ophthalmic Research 22, 271–279.
Söderberg, P.G., 1991. Na and K in the lens after exposure to radiation in the 300 nm wave length region. Journal of Photochemistry and Photobiology B 8, 279–294.
Söderberg, P.G., Chen, E., Lindström, B., 1990. An objective and rapid method for the determination of light dissemination in the lens. Acta Ophthalmologica (Copenh) 68, 44–52.
Söderberg, P.G., Löfgren, S., Ayala, M., Dong, X., Kakar, M., Mody, V., 2002. Toxicity of ultraviolet radiation exposure to the lens expressed by maximum tolerable dose (MTD). Developments in Ophthalmology 35, 70–75.
Söderberg, P.G., Michael, R., Merriam, J.C., 2003. Maximum acceptable dose of ultraviolet radiation: a safety limit for cataract. Acta Ophthalmologica Scandinavica 81, 165–169.
Söderberg, P.G., Philipson, B.T., Lindström, B., 1986. Unscheduled DNA synthesis in lens epithelium after in vivo exposure to UV radiation in the 300 nm wavelength region. Acta Ophthalmologica (Copenh) 64, 162–168.
Taylor, H.R., West, S.K., Rosenthal, F.S., Munoz, B., Newland, H.S., Abbey, H., Emmett, E.A., 1988. Effect of ultraviolet radiation on cataract formation. New England Journal of Medicine 319, 1429–1433.
Congdon, N., Vingerling, J.R., Klein, B.E., West, S., Friedman, D.S., Kempen, J., O'Colmain, B., Wu, S.Y., Taylor, H.R., 2004. Prevalence of cataract and pseudophakia/aphakia among adults in the United States. Archives of Ophthalmology 122, 487–494.
Thylefors, B., 1998. A global initiative for the elimination of avoidable blindness. American Journal of Ophthalmology 125, 90–93.
Vrensen, G.F.J.M., Sanderson, J., Willekens, B., Duncan, G., 1995. Calcium localization and ultrastructure of clear and pCMPS-treated rat lenses. Investigative Ophthalmology and Visual Science 36, 2287–2295.
Wegener, A.R., 1994. In vivo studies on the effect of UV-radiation on the eye lens in animals. Documenta Ophthalmologica 3–4, 221–232.
Wegener, A.R., 1995. In vivo studies on the effect of UV-radiation on the eye lens in animals. Documenta Ophthalmologica 88, 221–232.
West, S.K., 2000. Looking forward to 20/20: a focus on the epidemiology of eye diseases. Epidemiologic Reviews 22, 64–70.
West, S.K., Valmadrid, C.T., 1995. Epidemiology of risk factors for age-related cataract. Survey of Ophthalmology 39, 323–334.
Wu, K., Shui, Y., Kojima, M., Murano, H., Sasaki, K., Hockwin, O., 1997. Location and severity of UV-B irradiation damage in rat lens. Japanese Journal of Ophthalmology 41, 381–387.
Zhang, F., Löfgren, S., Söderberg, P.G., 2007. Interaction of anesthetic drugs and UVR-B irradiation in the anterior segment of the rat eye. Acta Ophthalmologica Scandinavica 85, 745–752.
Zigman, S., 1985. Photobiology of the lens. In: The Ocular Lens. Structure, Function and Pathology. Marcel Dekker, New York, pp. 301–347.
Zigman, S., Griess, G., Yulo, T., Schultz, J., 1973. Ocular protein alterations by near UV light. Experimental Eye Research 15, 255–264.